Liquid transport generated by a flashing field-induced wettability ratchet

Karin John[a)]
Laboratoire de Spectrométrie Physique, Université Joseph Fourier, Grenoble I, BP 87, 38402 Saint-Martin-d'Hères, France

Uwe Thiele[b)]
Max-Planck-Institut für Physik komplexer Systeme, Nöthnitzer Str. 38, D-01187 Dresden, Germany

(Received 16 April 2007; accepted 30 May 2007; published online 27 June 2007)

The authors develop a model for ratchet-driven macroscopic transport of a continuous phase. The transport relies on a field-induced dewetting-spreading cycle of a liquid film based on a switchable, spatially asymmetric, periodic interaction of the free surface of the film and the solid substrate. The concept is exemplified using an evolution equation for a dielectric liquid film under an inhomogeneous voltage. The authors analyze the influence of the various phases of the ratchet cycle on the transport properties. Conditions for maximal transport and the efficiency of transport under load are discussed. © *2007 American Institute of Physics*. [DOI: 10.1063/1.2751582]

Brownian ratchets present a well established way to induce directed motion of particles in spatially extended systems without global gradients, i.e., without a globally broken spatial symmetry.[1,2] Examples include colloidal particles suspended in solution that move in a sawtooth electric potential[3] and the selective particle filter formed by a microfabricated silicon membrane with asymmetrical bottlenecklike pores under application of an oscillating pressure gradient.[4,5] Brownian transport is based on the Curie principle,[6] stating that a macroscopically symmetric constellation may induce macroscopic transport if it exhibits local asymmetries, e.g., a periodic asymmetric potential that varies on a small length scale. However, the system has to be kept out of equilibrium, for instance, by an oscillating pressure[4] or electric potential.[3] In present applications, ratchets are mainly used to transport or filter discrete objects; however, they may also serve to induce transport of a continuous phase. Experimental observations include a secondary liquid flow triggered in Marangoni-Bénard convection involving a solid substrate with asymmetric grooves.[7] On a similar substrate Leidenfrost drops perform a directed motion.[8,9] Microdrops confined in asymmetrically structured geometries move when vibrating the substrate or applying an on/off electric field.[10]

In this letter we propose a simple model for ratchet-driven free-surface flow resulting in the macroscopic transport of a continuous phase. The driving flashing ratchet is based on a switchable, spatially periodic but asymmetric interaction of the liquid-gas interface and the solid substrate. A simple experimental setup consists of a thin film of dielectric liquid in a capacitor producing a periodic, spatially asymmetric voltage profile when switched on. Other choices, not pursued here, include switchable brushes, heating, or optical substrate properties. Although length and time scales and the interaction potential will differ, all these realizations can be mapped onto our model using appropriate pressure terms corresponding to effective switchable "wettabilities."

An idealized electrical wettability ratchet (sketched in Fig. 1) works as follows. A flat wetting film is stable in the absence of an electric field [Fig. 1(a)]. Upon switching on an electric field at $t=0$ [Fig. 1(e)] the film is destabilized by both, the overall electric field, and its local gradients [Fig. 1(d)]. This behavior is similar to dewetting on a heterogeneous substrate.[11] After a transient all the liquid is collected in drops at the locations of maximal voltage [Fig. 1(b)]. After switching off the field at $t=\tau$ [Fig. 1(e)], the drops spread into a homogeneous wetting layer [Fig. 1(c)] and at $t=T$ the cycle restarts.

For simplicity, we restrict our attention to a two-dimensional system, i.e., a shallow channel geometry, and neglect the influence of the channel walls. Using the lubrication approximation,[12] the ratchet dynamics can be captured by an evolution equation for the film thickness profile h,

$$\partial_t h = \partial_x \left[\frac{h^3}{3\eta} (\partial_x p - f_{\mathrm{ext}}) \right], \tag{1}$$

which is given by the divergence of the flow, expressed as the product of a mobility and a pressure gradient $\partial_x p$ and external force f_{ext} in x direction. η is the dynamic viscosity. The horizontal velocity component is $u(x,z)=(z^2/2-zh)\times[\partial_x p - f_{\mathrm{ext}}]$ and the vertical one results from continuity. The pressure

$$p = -\gamma \partial_{xx} h - \Pi(h,x,t) \tag{2}$$

contains the curvature pressure $-\gamma\partial_{xx}h$, where γ denotes surface tension and a generalized disjoining pressure $\Pi(h,x,t)$.

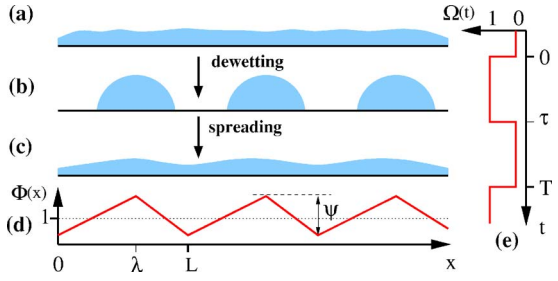

FIG. 1. (a)–(c) illustrate the working principle of a fluidic ratchet based on a switchable wettability that causes dewetting-spreading cycles. (d) depicts the spatial asymmetric periodic interaction profile $\Phi(x)$ responsible for the wettability pattern, and (e) indicates the time dependence $\Omega(t)$ of the switching in relation to the dewetting and spreading phases in (a)–(c).

a)Electronic mail: kjohn@spectro.ujf-grenoble.fr
b)Electronic mail: thiele@mpipks-dresden.mpg.de; URL: http://www.uwethiele.de

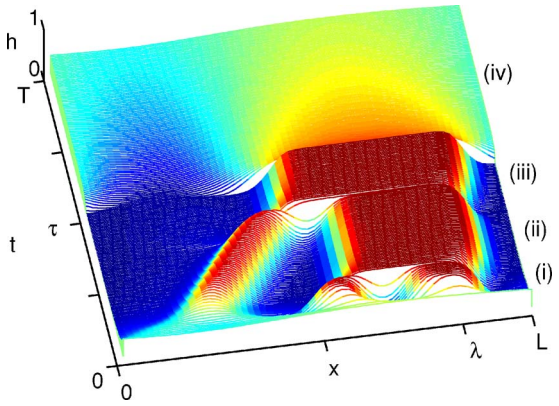

FIG. 2. Evolution of the film thickness profile of a dielectric liquid in a capacitor during one flashing period. Shown is one spatial period. Phases (i)–(iv) indicated at the right are explained in the main text. Parameters are $\bar{h}=0.5$, $\psi=0.5$, $L=32$, $\phi=5$, $T=5000$, $\omega=1$, $A=0.001$, $\varepsilon=2.5$, and $f_{\text{ext}}=0$. The starting time is well after initial transients have decayed.

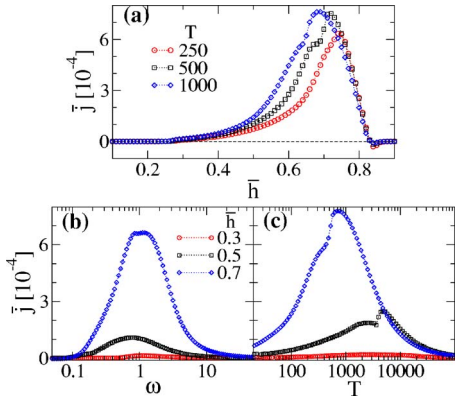

FIG. 3. Variation of $\bar{j}$ depending on (a) the mean film thickness ($\omega=1$), (b) the flashing ratio ω ($T=500$) and (c) the flashing period T ($\omega=1$) for various film thicknesses or flashing periods as given in the legends. The remaining parameters are as in Fig. 2.

The latter comprises all interactions between the free surface and the substrate, i.e., the effective wettability.[12,13] Note, that the lubrication approximation can be formally applied to systems involving small surface slopes only, but predicts the qualitative behavior for most systems with large contact angles.[12]

As model system we use a dielectric oil in a capacitor of gap width d and applied voltage U_0. The oil wets the lower plate and does not wet the upper plate corresponding to the van der Waals disjoining pressure

$$\Pi_{\text{vdW}} = \frac{1}{6\pi}\left(\frac{A_l}{h^3} + \frac{A_u}{(d-h)^3}\right), \tag{3}$$

with the Hamaker constants $A_l>0$ and $A_u<0$. The electrical "disjoining" pressure is[14,15]

$$\Pi_{\text{el}} = \frac{1}{2}\varepsilon_0\varepsilon_r U_0^2 \frac{(\varepsilon_r - 1)}{[\varepsilon_r d + (1-\varepsilon_r)h]^2}, \tag{4}$$

where ε_0 and ε_r are the absolute and relative dielectric constants, respectively. We assume $\varepsilon_{\text{gas}}=1$. The electric field is modulated in space ($\Phi(x)$) and time ($\Omega(t)$), as defined in Figs. 1(d) and 1(e), respectively, with $(1/L)\int_0^L \Phi(x)dx=1$. In consequence, Π in Eq. (2) is

$$\Pi(h,x,t) = \Omega(t)\Phi(x)\Pi_{\text{el}}(h) + \Pi_{\text{vdW}}(h). \tag{5}$$

To obtain a minimal set of parameters we introduce the scales $3\gamma\eta/d\kappa_{\text{el}}^2$, $\sqrt{\gamma d/\kappa_{\text{el}}}$, and d for t, x, and h, respectively. The electrostatic "spreading coefficient" is defined by $\kappa_{\text{el}}=\varepsilon_0\varepsilon_1 U_0^2/2d^2$. For simplicity we assume $A_u=-A_l$ and obtain the dimensionless Hamaker constant $A=A_l/6\pi d^3\kappa_{\text{el}}$. The resulting dimensionless equations correspond to Eqs. (1)–(5) with $3\eta=\gamma=d=\varepsilon_0\varepsilon_1 U_0^2/2=1$. They are analyzed numerically using an explicit scheme with periodic boundary conditions, complemented by the calculation of stationary solutions for $\Omega(t)=1$ using continuation.[16] All results are in dimensionless form. We introduce the asymmetry ratio $\phi=\lambda/(L-\lambda)$ and the flashing ratio $\omega=\tau/(T-\tau)$, characterizing the ratchet and quantify the resulting transport along the substrate by the mean flow $\bar{j}=(1/TL)\int_0^T dt\int_0^L dx j(x,t)$, where $j(x,t)=-h^3(\partial_x p - f_{\text{ext}})$.

Figure 2 shows a typical example of the film evolution during one ratchet cycle. One can distinguish four phases: (i) When the ratchet is switched on, the film is nearly flat but rapidly evolves a surface instability with a wavelength given approximately by the spinodal length.[12] In (ii), the evolving profile coarsens accelerated by the gradients of the ratchet potential until in (iii) only one drop remains, corresponding to the equilibrium structure on the heterogeneous wettability pattern.[11] (iv) After switching off the ratchet, the drop spreads under the influence of van der Waals forces until the next cycle starts. In the geometry introduced in Fig. 1 with $\phi>1$, each cycle transports liquid into the positive x direction.

The competing influence of the various parameters allows us to tune the transport. Figure 3 shows the mean flux $\bar{j}$ depending on the mean film thickness $\bar{h}$ and the temporal ratchet properties ω and T. The transport is strongest for intermediate $\bar{h}$, whereas for very small or large $\bar{h}$ the stabilizing van der Waals terms dominate and the mean flow approaches zero [Fig. 3(a)]. Figures 3(b) and 3(c) present the nonmonotonous dependencies of the flow on the flashing ratio ω and period T, respectively. For small ω the flow is practically zero, since the time for dewetting is too short to trap a considerable amount of liquid at the spots of high wettability. The flow increases with ω until reaching a maximum at $\omega\approx 1$. Beyond the maximum it decreases again because less and less time remains for spreading. The dependence on the flashing period T is similar but shows a particularly interesting nonmonotonous behavior close to the flow maximum. For small periods, the fluid has neither enough time to dewet nor to spread implying small mean transport. At large periods both processes reach the respective equilibrium well before the next switching, i.e., most time is spent waiting and the mean flow decreases approximately as $1/T$.

Note that a film of intermediate thickness in a homogeneous field ($\Phi(x)=\Omega(t)=1$) dewets spinodally with a wavelength well below the spatial period of the ratchet. Therefore the ongoing coarsening interacts with the flow induced by the ratchet and leads to the nonmonotonous behavior mentioned above. Further calculations (not shown) demonstrate the monotonous increase of $\bar{j}$ with increasing asymmetry ratio ϕ (with zero net transport at $\phi=1$) and the amplitude ψ of the ratchet potential.

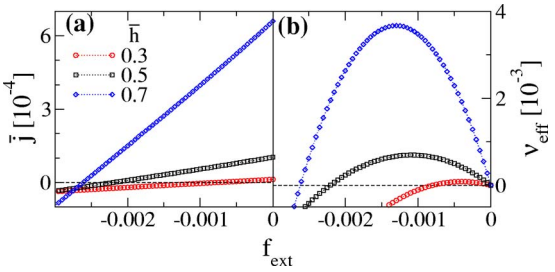

FIG. 4. Influence of an external load f_{ext}. Shown are the variations of (a) the mean flow $\bar{j}$ and (b) the transport efficiency ν_{eff} with f_{ext} for various mean film thicknesses $\bar{h}$, as indicated in the legends. The remaining parameters are as in Fig. 2 except for $T=500$. As an example, the force scale for water is 10^7 N m^{-3}.

Figure 4 shows the effect of an external force on the transport properties. Simple mechanical realizations of f_{ext} are an inclined substrate or centrifugal forces yielding a constant f_{ext}. The flashing ratchet under load ($f_{ext}<0$) generates a positive flow, i.e., mechanical work is performed against the external force, which can be characterized by the (mechanical) energy transport efficiency $\nu_{eff}=-\dot{W}/\dot{Q}$, where $\dot{W}=-\bar{j}f_{ext}$ and

$$\dot{Q}=\frac{1}{TL}\int_0^L dx\int_0^T dt\, h^3(\partial_x p-f_{ext})^2$$

denote the mechanical work performed and the energy dissipated per unit time, respectively. ν_{eff} [Fig. 4(b)] exhibits an optimum. For higher forces the flow reverses and the ratchet can no longer perform work against the external force. Note, that ν_{eff} is very small, since most energy is dissipated by viscous friction.

Finally, we discuss the feasibility of an electrical fluid ratchet by estimating the acting forces and relevant time and length scales for fluidic systems on various scales. Typical material constants for thin films in capacitors are taken from Ref. 15 and references therein. Applying a voltage of 100 V (10 V) over a gap of 2 mm (20 μm) width, a 1 mm (10 μm) film of silicon oil feels an electrostatic pressure of $p_{el}\approx 0.01$ Pa ($p_{el}\approx 1$ Pa) corresponding approximately to the curvature pressure in a drop of 1 mm (10 μm) height with $\theta_0=2°$ equilibrium contact angle. In principle, nanofluidic transport of polymer melts is also feasible. For a 30 nm film of liquid polystyrene in a capacitor with a 100 nm gap ($U_0=10$ V), $p_{el}\approx 10^4$ Pa equivalent to the curvature pressure for a droplet of 30 nm height and 300 nm width. Note, however, that for ultrathin films the disjoining pressure is of the same order of magnitude.[17] The time scale $\tau=3\gamma\eta/d\kappa_{el}^2$ reflects the relevant properties responsible for the relaxation toward the flat film. For a 5 cS silicon oil τ is between 1 and 100 s, i.e., the viscous flow is rather slow. However, in water films of thicknesses between 10 μm ($U_0=10$ V) and 1 mm ($U_0=100$ V) transport is fast with τ between 1 and 100 ms.

In conclusion, we have shown that a flashing ratchet produces a macroscopic transport in a liquid film with a free surface on a feasible time scale. There exist regimes of maximum transport selected by the spatial and temporal properties of the ratchet and depend on the characteristics of the thin film. For a spatial period of the ratchet considerably larger than the spinodal length scale of the film in a homogeneous field, the interaction of coarsening and ratchet-driven flow results in a nonmonotonous transport behavior.

This work was supported by the EU and DFG under Grant No. MRTN-CT-2004-005728 and SFB-486–B13, respectively. One of the authors (K.J.) was supported by grants from the CNES and the Humboldt-Foundation.

[1] R. D. Astumian and P. Hänggi, Phys. Today **55** (10), 33 (2002).
[2] P. Hänggi, F. Marchesoni, and F. Nori, Ann. Phys. **14**, 51 (2005).
[3] J. Rousselet, L. Salomé, A. Ajdari, and J. Prost, Nature (London) **370**, 446 (1994).
[4] S. Matthias and F. Müller, Nature (London) **424**, 53 (2003).
[5] C. Kettner, P. Reimann, P. Hänggi, and F. Müller, Phys. Rev. E **61**, 312 (2000).
[6] P. Curie, J. Phys. III (Paris) **3**, 393 (1894).
[7] A. D. Stroock, R. F. Ismagilov, H. A. Stone, and H. M. Whitesides, Langmuir **19**, 4358 (2003).
[8] D. Queré and A. Ajdari, Nat. Mater. **5**, 429 (2006).
[9] H. Linke, B. J. Aleman, L. D. Melling, M. J. Taormina, M. J. Francis, C. C. Dow-Hygelund, V. Narayanan, R. P. Taylor, and A. Stout, Phys. Rev. Lett. **96**, 154502 (2006).
[10] A. Buguin, L. Talini, and P. Silberzahn, Appl. Phys. A: Mater. Sci. Process. **75**, 207 (2002).
[11] U. Thiele, L. Brusch, M. Bestehorn, and M. Bär, Eur. Phys. J. E **11**, 255 (2003).
[12] A. Oron, S. H. Davis, and S. G. Bankoff, Rev. Mod. Phys. **69**, 931 (1997).
[13] P.-G. deGennes, Rev. Mod. Phys. **75**, 827 (1985).
[14] Z. Q. Lin, T. Kerle, S. M. Baker, D. A. Hoagland, E. Schäffer, U. Steiner, and T. P. Russell, J. Chem. Phys. **114**, 2377 (2001).
[15] D. Merkt, A. Pototsky, M. Bestehorn, and U. Thiele, Phys. Fluids **17**, 064104 (2005).
[16] E. Doedel, H. B. Keller, and J. P. Kernevez, Int. J. Bifurcation Chaos Appl. Sci. Eng. **1**, 745 (1991).
[17] J. N. Israelachvili, *Intermolecular and Surface Forces* (Academic, London, 1992).